

Spin-carrying spin polarons in the t - J model*

A. V. Dotsenko

School of Physics, The University of New South Wales, Sydney 2052, Australia

<mailto:dav@newt.phys.unsw.edu.au>

(May 18, 2019)

Abstract

The report discusses the spinless-fermion (holon) representation of the t - J model and describes a new analytical representation in which fermion operators are directly related to the physical electron operators and have spin. A simple, leading-order, treatment of the magnetic dynamics allows to take into account the spin-liquid aspect of the ground state. The obtained effective model, in comparison to that for holons, has an additional bare dispersion due to the hole moving by using quantum spin fluctuations present in the undoped antiferromagnetic ground state. The single-hole Green's function at half-filling is then found numerically using the self-consistent Born approximation. For all quantities studied good or excellent agreement with numerical data is observed in the entire parameter range, much improving on the holon results. Using the introduced formalism, the two-hole problem is also studied by solving numerically the Bethe-Salpeter equation with noncrossing diagrams. The applicability of the method for the more general many-body doped case and some other related issues are discussed.

I. INTRODUCTION

Much, if not most, of the progress in describing theoretically the complex physics of high-temperature superconductors and strongly correlated electrons has been achieved using numerical methods,¹ while analytical methods have been rather approximate (not for lack of trying) and not often checked against numerical data. A simple and transparent analytical or semianalytical model can however be very valuable by providing physical insights for *understanding* in addition to describing the system, by being easily extendible to other problems, and perhaps by being accessible to physicists without supercomputers:). Currently this is the role of the so-called self-consistent Born approximation,²⁻⁵ which provides a fairly good description of the undoped t - J model in the small J/t regime. More accurately, it is a

*The alternative title is *Born Again*. A politically correct version of this manuscript has been submitted to Phys. Rev. B.

holon-and-slave-boson representation⁶ of the t - J model in which (*i*) the boson part is treated to leading order in $1/S$ and (*ii*) the interacting holon-boson system is solved numerically using leading-order diagrams (for both *i* and *ii*, higher-order terms/diagrams have been analyzed by Liu and Manousakis⁵).

In this publication I report a modification to the scheme. The idea is to keep track of the hole's spin using *hole*, as opposed to *holon*, operators. It allows easily to take into account, if only on a mean-field basis, the quantum spin fluctuations present in the undoped ground state. The obtained effective model, consisting of interacting holes and spin waves, is the same as for holons and spin waves except for the presence of a bare hole dispersion due to the hole moving by eating away spin fluctuations present in the ground state. Solving the equations of motion for one hole in the self-consistent Born approximation, I find a fairly good agreement with numerical results for all analyzed quantities, such as the bandwidth and the band structure, and for all parameter regimes. The two-hole problem is also studied using the leading-order, noncrossing diagrams, demonstrating again viability of the method albeit much less convincingly.

In the following Sec. II, I describe what I call a spin-slave formulation of the t - J model. Then, in Sec. III the obtained results for single- and two-hole problems are compared against the available numerical data. The report ends with a summary (Sec. IV).

II. ANALYTICAL TRANSFORMATIONS OF THE t - J MODEL

The familiar t - J Hamiltonian is

$$H = -t \sum_{\langle ij \rangle \sigma} (c_{i\sigma}^\dagger c_{j\sigma} + \text{H.c.}) + J \sum_{\langle ij \rangle} \left(\mathbf{S}_i \cdot \mathbf{S}_j - \frac{1}{4} n_i n_j \right), \quad (1)$$

where the notation is standard with the addition that, both here and throughout the paper, n , i , and j refer to any, spin-up, and spin-down sublattice sites, respectively (n as a subindex is not to be confused with the electron number operators n_n). Recently, an extra t' term describing next-nearest-neighbor hopping is usually added to the model.⁷ This study however, being mainly for demonstrative and comparative purposes, is restricted to the original t - J model Eq. (1).

The Hamiltonian Eq. (1) is written without the commonly included electron projection operators on the understanding that, instead, the Hilbert space is restricted to no double electron occupancy (see Fig. 1). It is this constraint and that the electrons enter the Hamiltonian as both linear, $c_{n\sigma}$, and bilinear, \mathbf{S}_n , operators that makes the t - J Hamiltonian a very awkward one, badly suited for analytical study.

A. The holon-and-spin-slave formulation of the t - J model

To disentangle the Hamiltonian, the main degrees of freedom must be identified and suitable operators introduced. Intuitively, spin fluctuations and mobile holes are the main underlying objects. It was, to the best of my knowledge, Schmitt-Rink, Varma, and Ruckenstein⁶ who first proposed to represent the system as a combination of a spinless-fermion (holon) field and a slave boson field. (Somewhat paradoxically, the Hamiltonian is simplified by

introducing *extra* operators and degrees of freedom, instead of just ignoring some of them, which is what should be naively done.)

To make a bridge to the model proposed later, I give below an alternative but essentially the same description of the transformation. The difference is in using a slave *spin*, not *boson*, field. I believe it is more clear by virtue of separating the issue of separating magnetic and charge degrees of freedom from the issue of analyzing the spin field (the Holstein-Primakoff transformation, the spin-wave theory, etc). It is also more general and perhaps could be with few a modifications used when hopefully one day the phases with other than long-range-antiferromagnetic order/disorder can be described theoretically.

In the holon-and-slave-spin formulation, the t - J model Hilbert space Fig. 1 is mapped onto the one in Fig. 2. At any site n , there can be a holon h_n and there is always a slave spin \mathbf{s}_n . A “normal,” that is containing one electron, site is thought of as having no holon, while the spin field on such site is identified with the spin of the electron, $\mathbf{s}_n \equiv \mathbf{S}_n$ for $h_n^\dagger h_n = 0$. An empty site is considered to have one holon, while the spin field on it is declared to be up if the site is on the spin-up sublattice and down otherwise. This choice is motivated by the Ising limit.

Analytically, the most general form of the transformation is

$$c_{n\sigma} = h_n^\dagger \left(\frac{1}{2} \delta_{\sigma\sigma'} + \boldsymbol{\tau}_{\sigma\sigma'} \cdot \mathbf{s}_n \right) A_{n\sigma'}, \quad (2)$$

where $\boldsymbol{\tau}$ are the Pauli matrices and the transformation parameters satisfy $A_{n\sigma}^* A_{n\sigma} = 1$. The traditional form of the transformation, convenient for the antiferromagnetically-ordered phase, corresponds to $(A_{i\uparrow}, A_{i\downarrow}) = (1, 0)$ and $(A_{j\uparrow}, A_{j\downarrow}) = (0, 1)$. The relation for the spin operators is simply $\mathbf{S}_n = \mathbf{s}_n (1 - h_n^\dagger h_n)$.

In such analytical representation, by use of the half-filled state as the background, most correlations present in the system are already taken into account. Due to fermion statistics, it is automatically guaranteed that no more than one holon can be on a site. There is however an inconvenient constraint of no holon and a deviant spin coexisting on any site. (Being not very important in the undoped phase, it is generally either ignored or treated on a mean-field basis.)

Although introduced on intuitive grounds, the described transformation as such is exact. Certain approximations are introduced later, when the spin-wave theory is used to describe the spin field and $1/S$ expansion is made. Then some errors appear at the stage of solving the equations of motion for the already simplified Hamiltonian. However overall it appears that by far the main disadvantage of the method is that the holon is in only approximate correspondence to the hole. As discussed in the Appendix of Ref. 3, it is only when neglecting ground-state quantum spin fluctuations that the holon corresponds directly to a hole (or, to be more exact, to a simple linear combination of spin-up and spin-down holes). In the general case, a holon on any given site corresponds a mix of spin-up and spin-down holes. (Of course, there is no physical spin on a site when a hole is there. The spin of a hole is determined from the total spin of the lattice, or, in other words, by whether the hole was created by destroying a spin-up or a spin-down electron.) A direct way to rectify the mismatch is to use Eq. (2) to calculate the hole Green’s function from the known holon and magnon Green’s functions. In practice though such programme appears to be rather complicated. I show that there is an alternative straightforward scheme which uses the actual hole operators.

B. The hole-and-slave-spin approach to the t - J model

It is proposed here to describe the system as a combinations of a spin-and-charge carrying (spinful?) fermion field of holes $h_{n\sigma}$ and a slave spin field \mathbf{s}_n . The hole operators are the actual physical ones, a *direct* correspondence is made. Just like in the case of holons, when there is no hole the slave spin field is identified with the spin of the electron on the site, $\mathbf{s}_n \equiv \mathbf{S}_n$ for $h_{n\sigma}^\dagger h_{n\sigma} = 0$. In the half-filled state, the spin field \mathbf{s}_n is antiferromagnetically ordered, with a condensate of quantum spin fluctuations. When a hole is created, the slave spin field on that site is forced to be the opposite of the hole's spin, that is to be the spin of the destroyed electron. In subsequent processes, the dynamics of the slave spin is defined by the diagrams in Fig. 3. It is verified by direct analysis that the sum of the shown processes is equivalent to the hopping part of the t - J Hamiltonian. The logic behind these relatively complicated rules is clarified in Appendix A where an Ising-type situation is considered.

The form of the second part of the t - J Hamiltonian in this representation is trivial, the physical (or nonslave, or electron) spin field is represented as $\mathbf{S}_n = \mathbf{s}_n (1 - h_{n\sigma}^\dagger h_{n\sigma})$ and the electron occupation number operator as $n_n = 1 - h_{n\sigma}^\dagger h_{n\sigma}$ (summation over σ is implied). The definition of the representation is completed by the constraint of no double occupancy for holes.

At this point the Hamiltonian has only become more complicated. The idea however was that it can now be simplified significantly without loosing much accuracy. Ideally, it should be possible to forget about the approximations built into the model at this stage and focus on solving the effective Hamiltonian. If the transformation is “physically right,” or “natural” for the system, the leading-order results must be reasonably good. Fortunately, having numerical data allows to quickly test if this is so, at least in simple situations.

The guidance for the simplifications is that the spin fluctuations in the ground state are “few and far between.” The well-known characteristics of the Néel ground state are the staggered magnetization $m^\dagger = |\langle \psi_{\text{Néel}} | s_n^z | \psi_{\text{Néel}} \rangle| \approx 0.305$ and the nearest-neighbor spin correlator $e_{\text{AF}} = \langle \psi_{\text{Néel}} | \mathbf{s}_i \cdot \mathbf{s}_j | \psi_{\text{Néel}} \rangle |_{\langle ij \rangle} \approx -0.33$.

The first two processes in Fig. 3 describe the hole propagating by emitting and absorbing spin waves. These processes are the same as known for holons and I treat them to leading order in $1/S$. The last two processes of Fig. 3 describe the hole moving friction-free, by using the liquid component of the Néel state. In these terms I use replace spin combinations by their expectation values (*i.e.* do a mean-field/Hartree-Fock procedure where the inverse influence of the holes on the spin field is ignored). A relationship required here is

$$\langle \psi_{\text{Néel}} | \left(\left(\frac{1}{2} + s_i^z \right) \left(\frac{1}{2} + s_j^z \right) + s_i^+ s_j^- \right) | \psi_{\text{Néel}} \rangle = \frac{1}{4} + e_{\text{AF}}.$$

A caveat in writing the effective Hamiltonian is that for proper normalization, which is not absolutely necessary but convenient to have, the hole operators should actually be defined as $h_{n,-\sigma}^\dagger = \sqrt{2} c_{n\sigma}$, so that $\langle \psi_{\text{Néel}} | h_{\mathbf{k}\sigma} h_{\mathbf{k}\sigma}^\dagger | \psi_{\text{Néel}} \rangle = 1$ (no summation over σ). In the following, the following standard notation is used, $z = 4$ is the coordination number, N is the number of sites on the lattice, $\mathbf{Q} = (\pi, \pi)$, $\gamma_{\mathbf{k}} = \frac{1}{2}(\cos k_x + \cos k_y)$, and $\nu_{\mathbf{q}} = (1 - \gamma_{\mathbf{q}}^2)^{1/2}$.

With the described simplifications and after Fourier transformations, the effective Hamiltonian is

$$H_{\text{eff}} = \sum_{\mathbf{k}\sigma} E^{(0)}(\mathbf{k}) h_{\mathbf{k}\sigma}^\dagger h_{\mathbf{k}\sigma} + \sum_{\mathbf{q}} \omega_{\mathbf{q}} \alpha_{\mathbf{q}}^\dagger \alpha_{\mathbf{q}} + \frac{zt}{\sqrt{N}} \sum_{\mathbf{k}\sigma\mathbf{q}} M(\mathbf{k}, \mathbf{q}) (h_{\mathbf{k}\sigma}^\dagger h_{\mathbf{k}-\mathbf{q},\sigma} \alpha_{\mathbf{q}} + \text{H.c.})$$

$$+ \frac{1}{N} \sum_{\mathbf{k}\sigma\mathbf{k}'\sigma'\mathbf{q}} \Gamma_{\text{cont}}(\mathbf{q}) h_{\mathbf{k}'-\mathbf{q},\sigma'}^\dagger h_{\mathbf{k}+\mathbf{q},\sigma}^\dagger h_{\mathbf{k}\sigma} h_{\mathbf{k}'\sigma'}. \quad (3a)$$

The first term here, as a noticeable difference from the holon case, is a bare fermion dispersion

$$E^{(0)}(\mathbf{k}) = \left(\frac{1}{4} - e_{\text{AF}} \right) zJ - 2 \left(\frac{1}{4} + e_{\text{AF}} \right) zt\gamma_{\mathbf{k}}. \quad (3b)$$

The next two terms, describing spin waves with dispersion $\omega_{\mathbf{q}} = \frac{1}{2}zJ\nu_{\mathbf{q}}$ and interaction between holes and spin waves, are the same as in the holon case. The vertex function can be (conveniently?) written as

$$M(\mathbf{k}, \mathbf{q}) = \left[\frac{1}{2}(\nu_{\mathbf{q}}^{-1} + 1)\gamma_{\mathbf{k}-\mathbf{q}}^2 + \frac{1}{2}(\nu_{\mathbf{q}}^{-1} - 1)\gamma_{\mathbf{k}}^2 - \nu_{\mathbf{q}}^{-1}\gamma_{\mathbf{q}}\gamma_{\mathbf{k}}\gamma_{\mathbf{k}-\mathbf{q}} \right]^{1/2}. \quad (3c)$$

The last term, with

$$\Gamma_{\text{cont}}(\mathbf{q}) = \frac{1}{2} \left(e_{\text{AF}} - \frac{1}{4} \right) zJ\gamma_{\mathbf{q}}, \quad (3d)$$

may be called a “contact” interaction as it describes instantaneous attraction of holes on nearest-neighbor sites (easily recognized to be due to the “broken-bond” mechanism). This interaction is also present in the holon case but usually omitted since it is negligible in the usually considered regime of $J/t \ll 1$ and completely irrelevant in the single-hole problem.

It is trivially seen that the holon model is recovered when switching off the bare hole dispersion except that there are now twice as many fermionic degrees of freedom. Of course, due to the constraint the *total* number of fermions allowed in the system is the same N but there are now $2N$ states in the single-fermion sector. The missing holon degrees of freedom are accounted for by the slave spin/boson field. In the hole approach the total slave spin of the lattice in the state with one hole is always the same as in the hole-free state, while for holons it may have two values depending on whether the holon was created by destroying a spin-up or a spin-down electron.

The advantage of the present formulation, apart from the purely esthetic one of working with the actual physical operators, is that it very easily accounts for ground-state fluctuations by means of simply introducing a bare dispersion. The linear-in- t hole dispersion in the static limit has been known for some time.⁸ It may be obtained directly by calculating the amplitudes

$$\left\langle \psi_{\text{N\'eel}} \left| c_{i\sigma}^\dagger \left(t \sum_{\sigma'} c_{j\sigma'}^\dagger c_{i\sigma'} \right) c_{j\sigma} \right| \psi_{\text{N\'eel}} \right\rangle,$$

and remembering to normalize hole operators. What is remarkable is that this effect can be added “linearly” to the spin-wave-emission mechanism.

Note here that the linear-in- t hole dispersion is not a contradiction to a $\sim t^2/J$ bandwidth for *holons*. To zeroth approximation, the holon $h_{\mathbf{k}}$ is a combination of $h_{\mathbf{k}\downarrow} + h_{\mathbf{k}+\mathbf{Q},\downarrow}$ (spin-down holes on the spin-up sublattice, taking the origin to be on this sublattice) and $h_{\mathbf{k}\uparrow} - h_{\mathbf{k}+\mathbf{Q},\uparrow}$ (spin-up holes on the spin-down sublattice). The $\propto t\gamma_{\mathbf{k}}$ dispersion for holes obviously cancels out for holons. It means that a holon can be thought of as having four components which can travel but in opposite directions so that the holon as a whole (the “center of mass”) remains stationary.

The representation of a holon as having four components, strictly valid when ground-state fluctuations are ignored but approximately valid always, may explain why some of the quantities were in very good agreement with numerical data in the holon studies as well. For example as discussed above, the holon with $\mathbf{k} = (\pi/2, \pi/2)$ is to a good approximation a combination of holes with $\mathbf{k} = (\pi/2, \pi/2)$ and $\mathbf{k} = (-\pi/2, -\pi/2)$, so that the position of the quasiparticle pole and its residue will be similar. Except for $X = (\pi, 0)$, the situation is different for other points in the Brillouin zone.

It should also be possible to obtain the same effective Hamiltonian Eq. (3) by a direct rearranging of the terms in the t - J Hamiltonian Eq. (1).

III. COMPARISON OF RESULTS

A. The single-hole problem

To find the single-hole Green's function given the effective Hamiltonian Eqs. (3) it appears natural to use the same self-consistent Born approximations as in the holon case. The first crossing diagram¹ Fig. 4 is prohibited by kinematic reasons (it may be seen when the two-sublattice formalism is used that the spin wave emitted when the hole jumps from i to j must be absorbed when the hole jumps from j' to i'). The no-double-occupancy constraint in the single-hole problem is irrelevant. The Green's function is then found by solving the following Dyson equation (corresponding to the diagram in Fig. 5)

$$[G(\mathbf{k}, \omega)]^{-1} = [G^{(0)}(\mathbf{k}, \omega)]^{-1} - \frac{(zt)^2}{N} \sum_{\mathbf{q}} M^2(\mathbf{k}, \mathbf{q}) G(\mathbf{k} - \mathbf{q}, \omega - \omega_{\mathbf{q}}). \quad (4)$$

where $G^{(0)}(\mathbf{k}, \omega) = [\omega - E^{(0)}(\mathbf{k}) + i0]^{-1}$ is the zeroth order Green's function and integration over spin-wave frequencies has been carried out using the observation that in the single-particle case all poles of $G(\mathbf{k}, \omega)$ are in the lower plane.

In Figs. 6, 7, and 8, the solution of Eq. (4) on a 4×4 lattice is compared against exact results (I used data from Refs. 8 and 9). The agreement can be rated as good to excellent. Other quantities, such as the structure of the spectral function, were in good agreement too. Note also that since no account was taken of small-cluster specifics, such as a slightly different magnetic order and a relatively large influence of the hole on the spin order (very roughly speaking, one hole on a 4×4 lattice constitutes a sizeable 6% doping), it may be conjectured that the method is even more accurate than may be suggested by the given comparison. That the agreement is not an artifact of the highly degenerate 4×4 lattice is proved in Fig. 9, where the dispersion relation is compared to that obtained by the Green's function Monte Carlo method on the 16×16 lattice. In examining the accuracy it should

¹ For the interested reader, this and other diagrams in this report were produced using a fairly new L^AT_EX package **feynMF** (stands for Feynman METAFONT) by Thorsten Ohl (Technische Hochschule Darmstadt). The package is available from the Comprehensive T_EX Archive Network (<ftp.dante.de>, <ftp.shsu.edu>, <ftp.tex.ac.uk> and mirrors throughout the world). I highly recommend it to everyone dealing with Feynman diagrams.

also be remembered that physically the low-energy part of the band is most important (the close agreement for the quasiparticle residue at the band bottom is thus most encouraging).

Since the computational load is quite low, it is easy to move on to fairly large lattices. Finite-size effects per se almost disappear starting from the 8×8 lattice. The main drawback of small clusters seems to be a lack of resolution in \mathbf{k} space (however in the case of dispersion, a very smooth function, it can be mostly overcome by using trigonometric-function fits).

The dispersion relation calculated on a 32×32 lattice is shown in Figs. 10 and 11. Of course, the most notable difference from the holon case is that there is no degeneracy between \mathbf{k} and $\mathbf{k} + \mathbf{Q}$. In the low-energy part of the band there is now an extended nearly flat region near $X = (\pi, 0)$. This is in agreement with the experimental ARPES data and is probably key to explaining some of the experimental properties of the cuprates.¹¹

Another effect observed in the results is that the band minimum slightly shifts away from $\bar{M} = (\pi/2, \pi/2)$ towards $M = (\pi, \pi)$ while the maximum splits, moving from $\Gamma = (0, 0)$ in the direction of $X = (\pi, 0)$. Using various lattices and supplementing it with interpolation by means of trigonometric-functions fits, I found the minimum to be at $(0.503\pi, 0.503\pi)$ for $J/t = 0.4$ and at $(0.545\pi, 0.545\pi)$ for $J/t = 1$.

Higher-order terms will probably lead to a renormalization of the values of t and J , similar to what was found in the holon case.⁵ In the present study, the shape of the dispersion is almost the same in a fairly wide parameter range and is presumably very accurate but the absolute numbers may change.

B. The two-hole problem

As a further test of the method's usefulness, I applied it to the two-hole problem. Many issues that come up here are the same as in the many-body problem and, again, availability of some numerical data makes it a good opportunity to test viability and/or accuracy of the diagrammatic approach in a context more complex than the single-particle one. To the best of my knowledge, no such test has been made in the holon picture either and I believe this problem must be definitively solved analytically before attacking the many-body problem. All the following consideration is restricted to singlet pairs with total momentum zero.

The bound state is found by solving the Bethe-Salpeter equation

$$G_{\uparrow\downarrow}(\mathbf{k}, \omega) = \frac{1}{2\pi N} \sum_{\mathbf{k}'} \int d\omega' V(\mathbf{k}, \mathbf{k}', \omega - \omega') G(\mathbf{k}', E + \omega') G(-\mathbf{k}', E - \omega') G_{\uparrow\downarrow}(\mathbf{k}', \omega'), \quad (5)$$

where E is half the total energy (*i.e.* the energy *per hole*) and $G_{\uparrow\downarrow}(\mathbf{k}, \omega)$ is essentially the anomalous Green's function. For the four-particle scattering amplitude I used

$$V(\mathbf{k}, \mathbf{k}', \omega) = (zt)^2 M(\mathbf{k}, \mathbf{k} - \mathbf{k}') M(\mathbf{k}', \mathbf{k}' - \mathbf{k}) D(\mathbf{k} - \mathbf{k}', \omega) + \Gamma_{\text{cont}}(\mathbf{k} - \mathbf{k}'),$$

where $D(\mathbf{q}, \omega) = 2\omega_{\mathbf{q}}(\omega^2 - \omega_{\mathbf{q}}^2 + i0)^{-1}$ is the magnon Green's function. Note that the product of M 's is simply $[\gamma_{\mathbf{k}}\gamma_{\mathbf{k}'} - \frac{1}{2}\gamma_{\mathbf{q}}(\gamma_{\mathbf{k}}^2 + \gamma_{\mathbf{k}'}^2)]\nu_{\mathbf{q}}^{-1}$. This amplitude corresponds to the leading-order spin-wave exchange diagram and the contact interaction, which is all diagrammatically represented in Fig. 12. In the present single-lattice formulation spin waves do not change the spin of the hole.

In solving Eq. (5), the convolution over frequencies was performed using fast Fourier transforms (FFT), taking in various regimes 1024 to 8192 points for the frequency mesh. The frequency cutoff was typically $8t + 3J$. Although despite appearances the structure of the vertex allows FFT over momenta as well, doing so in practice involves fairly large overheads and small lattices are solved faster by direct summation in \mathbf{k} space, using all available symmetries. The bound state energy is found as the E at which (the real part of) the largest eigenvalue for a given symmetry becomes equal to 1 (the imaginary part was kept under 0.05 and its negligible influence was verified). The binding energy per pair is then $\Delta_B = 2(E - E_{\min})$, where E_{\min} is the minimum single-hole energy (by convention this must be found from the momenta actually available on the cluster instead of by interpolation or by using the bulk limit result).

The solution I consider is even in frequency and has a $d_{x^2-y^2}$ -wave spatial symmetry. In this case the configurations with two holes on a site are prohibited by the symmetry. (To enforce the constraint in the general case, it is quite easy to introduce a Hubbard-like repulsion of holes on the same site.)

The results, presented in Fig. 14, show a maybe-satisfactory agreement with numerical data. The dependence on J/t is noticeably different. The size dependence is matched rather well, suggesting that the difference is due to a “renormalization.” This is further illustrated in Fig. 15, where the result for obtained on the 16×16 lattice is also plotted, demonstrating almost complete finite-size convergence on such sizes.

Barring the possibility of an error, the most likely cause of the discrepancy is contribution of higher-order diagrams.¹⁶ In the regime of small t/J , the calculated binding energy behaves as square of the quasiparticle residue, which is what is expected but which is not what is seen in numerical data. The small size of the bound state may mean that a real-space based approach may be more efficient as the complexity of diagrams grows very quickly. The next-order omitted diagrams are shown in Fig. 13. The first crossing diagram, however, is expected to be zero for the same kinematic reason as in the single-hole case.¹⁷

Note also that the binding energy is quite small relative to the total energy scale. The result is very sensitive to values of interaction and the values of single-hole energy. Given the complexity of the problem, renormalizing the interaction is an attractive option.

Various features of the two-hole bound state have been discussed at length in the literature (see Ref. 1 and references therein, recent references are Refs. 14 and 15) and will not be described here except for a note on the “static” nature of the bound state. In the most naive, “nonrelativistic,” static limit the spin-wave Green’s function is replaced by $-2\omega_{\mathbf{q}}^{-1}$, thus creating a potential interaction. A more accurate approximation is to take into account holes’ velocity but assume a static wave function, $G_{\uparrow\downarrow}(\mathbf{k}, \omega) = G_{\uparrow\downarrow}(\mathbf{k}, \omega = 0) \equiv \Psi(\mathbf{k})$. This approach, used in several studies of the t - J model,¹⁸ is based on the following argument. Since the vertex function $M(\mathbf{k}, \mathbf{q})$ is small for small q , the *typical* energy of magnons involved in spin-wave exchange is of the order of $2J$. On the other hand, the energy scale for holes excitations [the scale of $G(\mathbf{k}, E + \omega)G(-\mathbf{k}, E - \omega)$] is $\frac{1}{2}(|\Delta_B| + W_{\text{eff}})$, where the effective hole bandwidth is $W_{\text{eff}} \sim 0.3t$, so that even at $J/t \sim 0.4$ the holes may be regarded as very slow. The results of solving the static version of the Bether-Salpeter equation

$$\Psi(\mathbf{k}) = \frac{1}{2\pi N} \sum_{\mathbf{k}'} \int d\omega' V(\mathbf{k}, \mathbf{k}', -\omega') G(\mathbf{k}', E + \omega') G(-\mathbf{k}', E - \omega') \Psi(\mathbf{k}') \quad (6)$$

at $J/t = 0.4$ are shown in Fig. 15. They show that the static approximation, of course far

from being completely safe, should be sufficient for most estimations, especially considering that errors introduced this way seem to be less than those originating from other sources (presumably from neglecting or mean-field-decoupling higher-order diagrams).

IV. SUMMARY

I have presented a variation of the well-known holon-and-slave-fermion approach allowing easily to take into account spin fluctuations present in the ground state. While the holon approach starts from the Ising state perturbatively puts holons and spin waves into it, in the present formulation first the magnetic order is found and *then* the hole motion is studied, so that self-consistency is achieved in the leading order. The results for single-hole properties within noncrossing-diagram approximation are found to be in good agreement with numerical data. The results clarify the nature of the hole dynamics. It is almost completely described by only two kinds of underlying processes: (*i*) a string-picture-like motion by means of emitting/absorbing a spin wave at each step and (*ii*) direct hopping on ground-state spin fluctuations.

The results for the two-hole problem are less clear and more work may be required.

In the physical regime of small J/t , the numerical differences of the holon formulation, from the presented method are fairly small. However since the described method has exactly the same level of complexity (or rather simplicity), there is no reason not to use it. A potential problem with applying the method to the doped case is the constraint of no double occupancy. In the single-hole problem the constraint is irrelevant, while in the two-hole one it happens to be irrelevant too. In the most general case, an on-site repulsion can be introduced. It will be however hard to define a Fermi surface as no simple filling of a band can occur, any hole created prohibits another hole being created at the same momentum.

ACKNOWLEDGMENTS

The author is supported from an Australian Research Council grant.

APPENDIX A: THE MOTION OF A HOLE ON AN ISING-TYPE BACKGROUND

In this Appendix I describe the hole motion in the presence of ground-state spin fluctuations using a very easy, one-dimensional Ising system. In the following, all even sites have been rotated by π .

The perfect antiferromagnetic ground state is shown in Fig. 16, and the motion of a hole in such background is depicted in Fig. 17. As the hole moves, it leaves behind a trail of flipped spins (although in one dimension they all amount to one spin-order distortion at the origin). The hole may move back to wipe out the distortion it created. In the corresponding two-dimensional, string picture, the hole creates a spin distortion at *each* step away from the origin. This is the essence of the holon approach in its standard formulation: The hole moves by either emitting a spin wave or by absorbing one that it created earlier. The spin wave can be thought of as a complex spread out in space form of spin flip/distortion, conceptually

the two are the same. Notice that the slave spin field on the hole site is left effectively idle, always being nonflipped according to the convention.

Now assume that for whatever reason (perhaps due to a kind of frustration) the ground state has the form in Fig. 18, that is it has spin flips/fluctuations frozen in it (incidentally, the flips come in pairs). On this background, in addition to the processes shown earlier in Fig. 17, there will be occasional processes where the hole moves without creating any new spin distortions, but only shifting those already present (Fig. 19). Analyzing the process in Fig. 19, an inconvenience of the holon approach becomes obvious. Namely, it is that although no actual spin excitation was created, there is a spin flip in the slave spin field due to rigidity of the slave spin attached to the holon. This makes the analytical transformation unnatural and it will be hard to account for such processes accurately. The easy way out is to fully employ the slave spin field by forcing it flip when necessary, thus carrying much more information and doing much more work. It will also be convenient (and necessary) to keep track of the hole's spin. Figure 20 illustrates the motion of a hole as described by the new conventions. The direction of the spin field together with the spin of the hole effectively indicates whether any encountered spin flip could have been created by the hole back in time or if it is a background spin fluctuation. In the latter case, the hole advances to the next site free—no strings attached.

REFERENCES

- ¹ E. Dagotto, Rev. Mod. Phys. **66**, 763 (1994).
- ² C. L. Kane, P. A. Lee, and N. Read, Phys. Rev. B **39**, 6880 (1989).
- ³ G. Martínez and P. Horsch, Phys. Rev. B **44**, 317 (1991).
- ⁴ F. Marsiglio, A. E. Ruckenstein, S. Schmitt-Rink, and C. Varma, Phys. Rev. B **43**, 10882 (1991).
- ⁵ Z. Liu and E. Manousakis, Phys. Rev. B **44**, 2414 (1991); Phys. Rev. B **45**, 2425 (1992); Phys. Rev. B **51**, 3156 (1995). I am grateful to M. Boninsegni for pointing out the last of these references.
- ⁶ S. Schmitt-Rink, C. M. Varma, and A. E. Ruckenstein, Phys. Rev. Lett. **60**, 2793 (1988).
- ⁷ O. K. Andersen, A. I. Liechtenstein, O. Jepsen, and F. Paulsen, J. Phys. Chem. Solids **56**, 1573 (1995).
- ⁸ E. Dagotto *et al.*, Phys. Rev. B **41**, 9049 (1990).
- ⁹ T. Barnes, A. E. Jacobs, M. D. Kovarik, and W. G. Macready, Phys. Rev. B **45**, 256 (1992).
- ¹⁰ M. Boninsegni, Phys. Lett. A **188**, 330 (1994).
- ¹¹ E. Dagotto, A. Nazarenko, and M. Boninsegni, Phys. Rev. Lett. **73**, 728 (1994).
- ¹² T. Barnes and M. D. Kovarik, Phys. Rev. B **42**, 6159 (1990).
- ¹³ M. Boninsegni and E. Manousakis, Phys. Rev. B **47**, 11897 (1993).
- ¹⁴ S. R. White and D. J. Scalapino, preprint [cond-mat/9605143](http://arxiv.org/abs/cond-mat/9605143).
- ¹⁵ V. I. Belinicher, A. L. Chernyshev, and V. A. Shubin, preprint [cond-mat/9611001](http://arxiv.org/abs/cond-mat/9611001).
- ¹⁶ Another potential reason for discrepancy is more subtle. Consider for example the case of $J/t \rightarrow 0$. In solving the problem analytically, it is easy to generate a very large number of virtual spin waves, while in fact physically it is clear that the number has to be less than the number of lattice sites. The diagrammatic approach is inherently for the bulk limit, which means that a direct comparison is not always possible. The actual criterion for agreement should be then that when no finite size effects are found in numerical data, then the results must agree. Otherwise the procedure is undefined, and some conclusions can only be drawn indirectly.
- ¹⁷ This observation is due to O. Sushkov.
- ¹⁸ M. Y. Kuchiev and O. P. Sushkov, Physica C **218**, 197 (1993); Phys. Rev. B **52**, 12977 (1995); V. I. Belinicher, A. L. Chernyshev, A. V. Dotsenko, and O. P. Sushkov, Phys. Rev. B **51**, 6076 (1995). Note that in these works $h_{\mathbf{k}\sigma}$ denotes a quasiparticle operator.

FIGURES

FIG. 1. The Hilbert space in the t - J model. The arrows represent electrons.FIG. 2. The Hilbert space in the t - J model as represented in the holon formulation. The arrows represent the (slave) spin field, while the circles show holons.FIG. 3. Graphical representation of the hopping part of the t - J Hamiltonian in the hole-and-slave-spin formulation. The large arrows are for the spin field, the small ones show the hole. The processes for the spin-up hole are similar, they are obtained by replacing $i \leftrightarrow j$.FIG. 4. The leading-order crossing diagram. i and j are sublattice indices.

FIG. 5. The Dyson equation for the single-hole Green's function in the self-consistent Born approximation.

FIG. 6. Quasiparticle bandwidth W on a 4×4 lattice.FIG. 7. Quasiparticle band structure on a 4×4 lattice. The lines are trigonometric-function fits to the points plotted. See Fig. 6 for the actual scale. Note there is no degeneracy between \mathbf{k} and $\mathbf{k} + \mathbf{Q}$ observed for holons.FIG. 8. The quasiparticle residue Z at the point $\bar{M} = (\pi/2, \pi/2)$ on a 4×4 lattice.FIG. 9. Quasiparticle band structure at $J/t = 0.4$ on a 16×16 lattice. The solid line (the result of the present work) was smoothed by constructing a trigonometric-function fit and it passes through all the points actually calculated. The real scales are somewhat different, $E(\Gamma) - E(\bar{M}) = 1.18t = 2.95J$ for the Green's function Monte Carlo result¹⁰ and $E(\Gamma) - E(\bar{M}) = 0.83t = 2.08J$ for the result of the present study.FIG. 10. The quasiparticle band structure at representative values of J/t . The result was obtained using a 32×32 lattice. The actual scales are as follows. For $J/t = 0.2$, $E(\Gamma) - E(\bar{M}) = 0.45t$; for $J/t = 0.4$, $E(\Gamma) - E(\bar{M}) = 0.83t$; for $J/t = 1$, $E(\Gamma) - E(\bar{M}) = 1.40t$. See also Fig. 11.FIG. 11. A three-dimensional plot of the “normalized” dispersion at $J/t = 0.4$.FIG. 12. The diagrams included in the four-particle scattering amplitude $V(\mathbf{k}, \mathbf{k}', \omega)$. The next-order omitted diagrams are shown in the following Fig. 13.

FIG. 13. The higher-order diagrams for the four-particle scattering amplitude. Both diagrams are expected to be suppressed (see the text).

FIG. 14. The two-hole binding energy Δ_B as a function of t/J . The numerical results on the 4×4 lattice are from exact diagonalizations. The numerical results on the 8×8 lattice are from Monte Carlo studies (Barnes and Kovarik¹² for $t/J = 0$ and Boninsegni and Manousakis¹³ for the other points). The numerical result on the 6×8 lattice was quoted by White and Scalapino¹⁴ in a density matrix renormalization group study. The analytical result is from Ref. 15. The irregularities at small t/J on the 4×4 lattice are caused by level crossings (at $t/J = 0.4814$ and 0.1526 , see Ref. 9).

FIG. 15. Size dependence of the two-hole binding energy Δ_B at $J/t = 0.4$. $L \times L$ is the lattice size. The dotted line is the result obtained using the static approximation described in the text.

FIG. 16. The perfectly antiferromagnetic ground state.

FIG. 17. Motion of a holon in perfectly antiferromagnetic background.

FIG. 18. An antiferromagnetic ground state with spin fluctuations present.

FIG. 19. Motion of a holon encountering a ground-state spin fluctuation.

FIG. 20. Motion of a hole in a background with spin fluctuations, as interpreted in the hole-and-slave-spin representation.

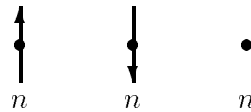


FIG. 1. The Hilbert space in the t - J model. The arrows represent electrons.

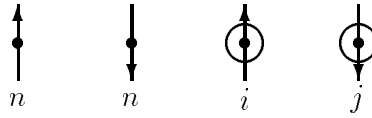


FIG. 2. The Hilbert space in the t - J model as represented in the holon formulation. The arrows represent the (slave) spin field, while the circles show holons.

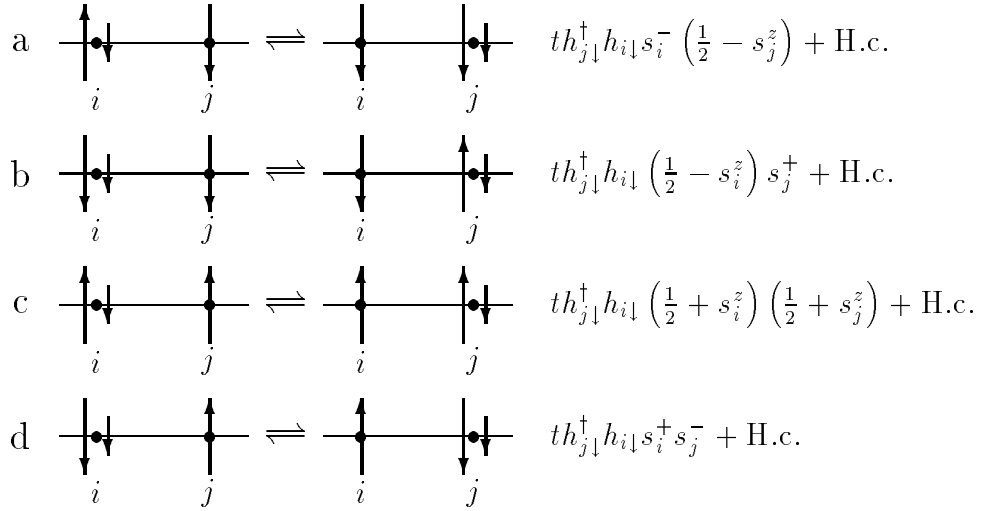


FIG. 3. Graphical representation of the hopping part of the t - J Hamiltonian in the hole-and-slave-spin formulation. The large arrows are for the spin field, the small ones show the hole. The processes for the spin-up hole are similar, they are obtained by replacing $i \leftrightarrow j$.

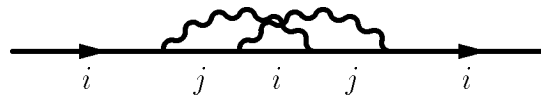


FIG. 4. The leading-order crossing diagram. i and j are sublattice indices.

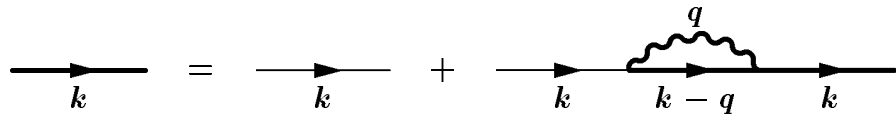


FIG. 5. The Dyson equation for the single-hole Green's function in the self-consistent Born approximation.

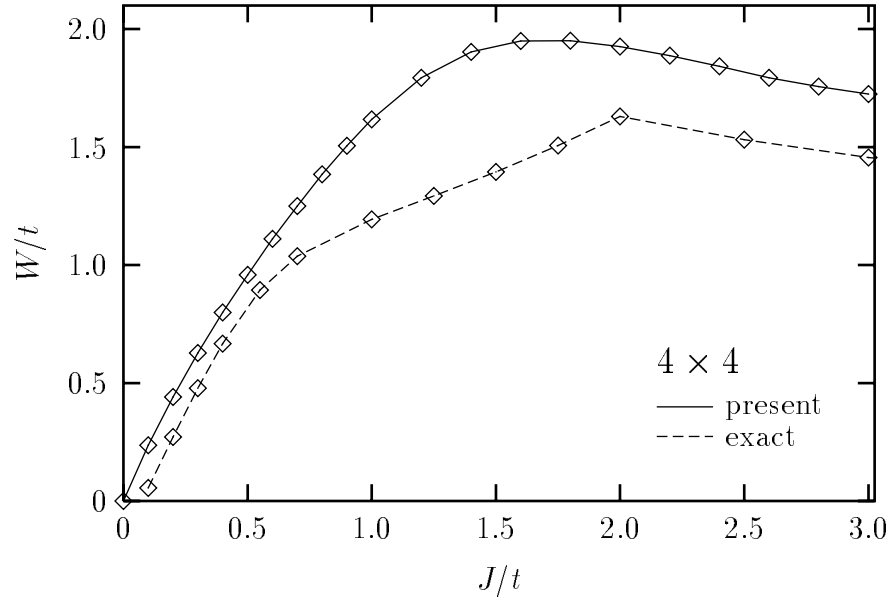


FIG. 6. Quasiparticle bandwidth W on a 4×4 lattice.

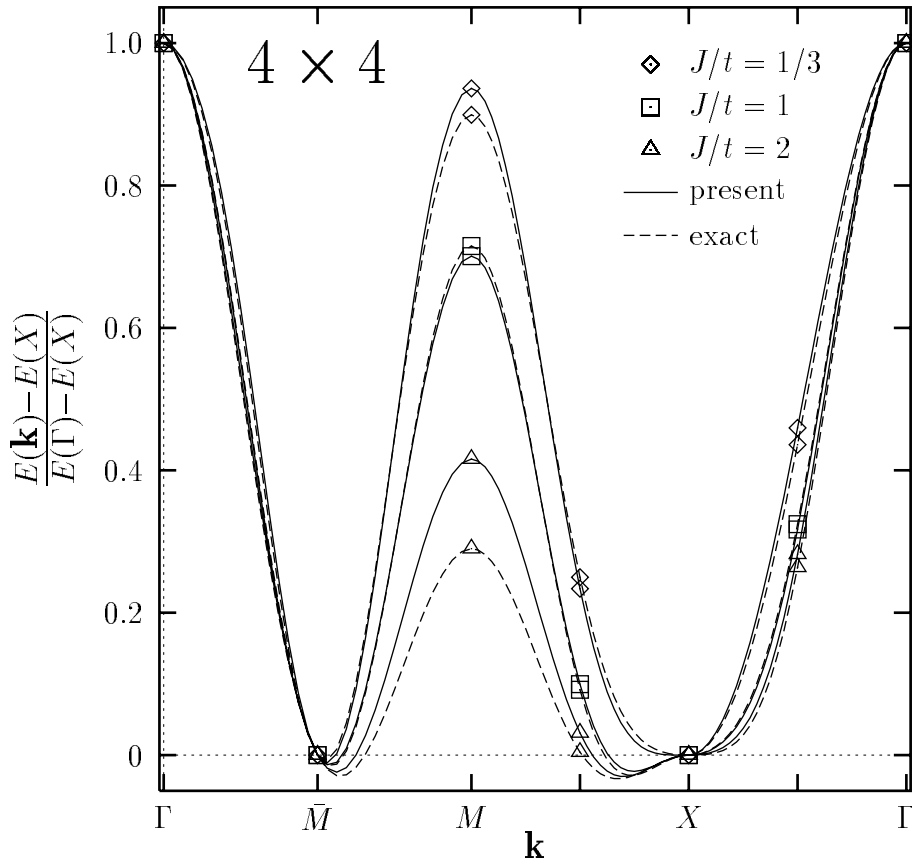


FIG. 7. Quasiparticle band structure on a 4×4 lattice. The lines are trigonometric-function fits to the points plotted. See Fig. 6 for the actual scale. Note there is no degeneracy between \mathbf{k} and $\mathbf{k} + \mathbf{Q}$ observed for holons.

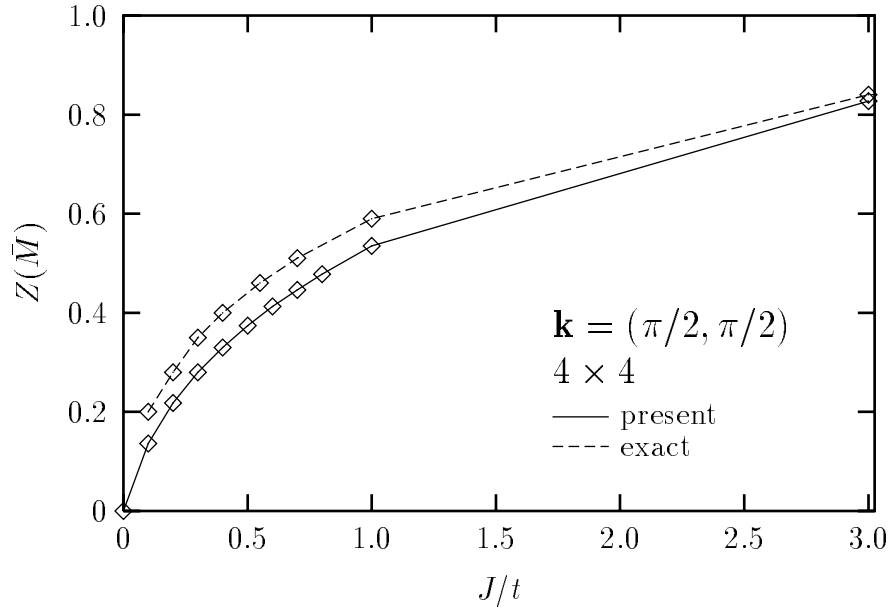


FIG. 8. The quasiparticle residue Z at the point $\bar{M} = (\pi/2, \pi/2)$ on a 4×4 lattice.

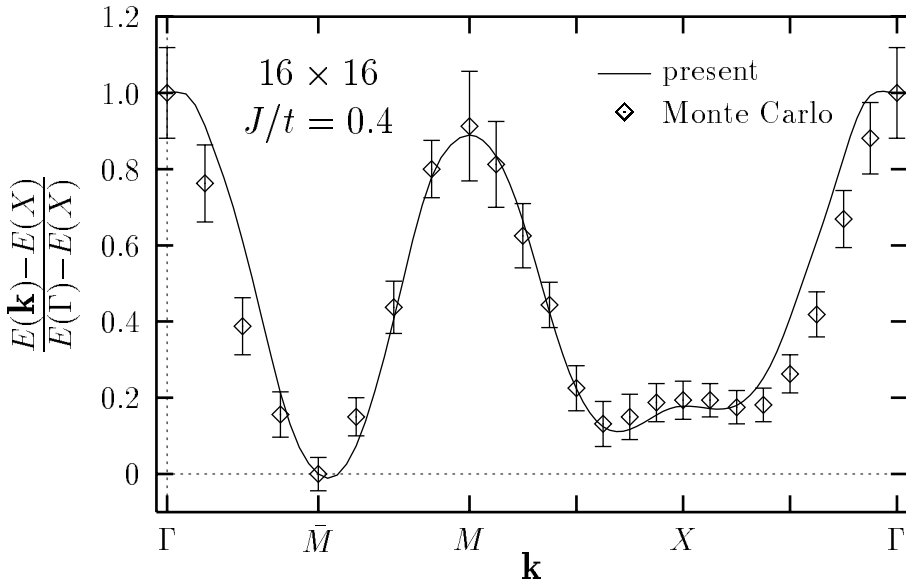


FIG. 9. Quasiparticle band structure at $J/t = 0.4$ on a 16×16 lattice. The solid line (the result of the present work) was smoothed by constructing a trigonometric-function fit and it passes through all the points actually calculated. The real scales are somewhat different, $E(\Gamma) - E(\bar{M}) = 1.18t = 2.95J$ for the Green's function Monte Carlo result¹⁰ and $E(\Gamma) - E(\bar{M}) = 0.83t = 2.08J$ for the result of the present study.

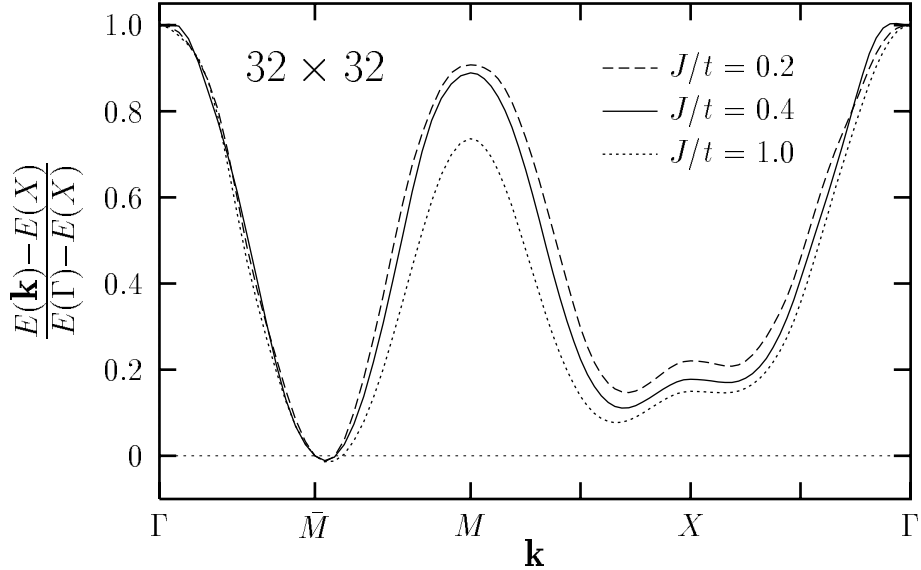


FIG. 10. The quasiparticle band structure at representative values of J/t . The result was obtained using a 32×32 lattice. The actual scales are as follows. For $J/t = 0.2$, $E(\Gamma) - E(\bar{M}) = 0.45t$; for $J/t = 0.4$, $E(\Gamma) - E(\bar{M}) = 0.83t$; for $J/t = 0.2$, $E(\Gamma) - E(\bar{M}) = 1.40t$.

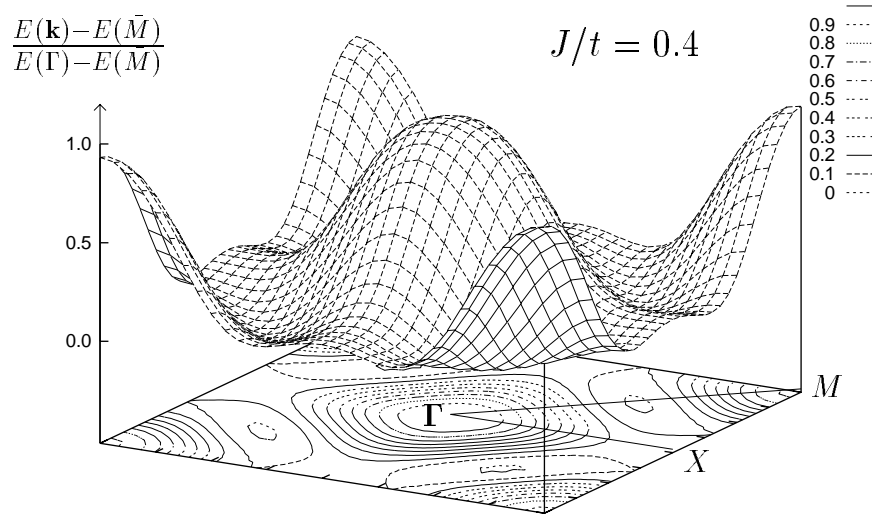


FIG. 11. A three-dimensional plot of the “normalized” dispersion at $J/t = 0.4$.

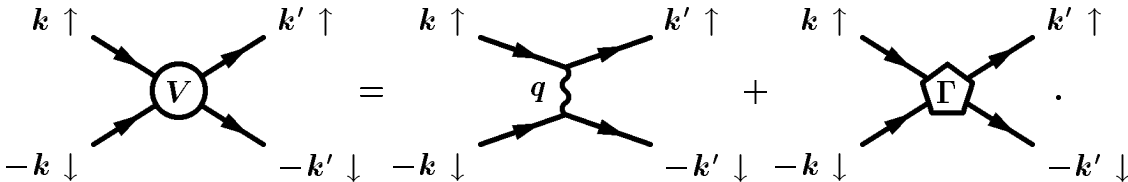


FIG. 12. The diagrams included in the four-particle scattering amplitude $V(\mathbf{k}, \mathbf{k}', \omega)$. The next-order omitted diagrams are shown in the following Fig. 13.

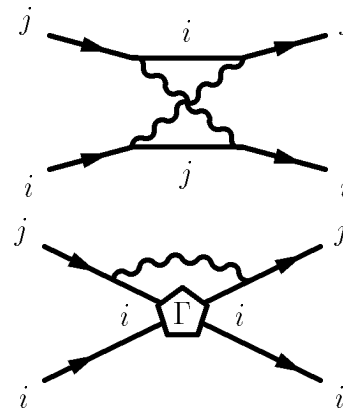


FIG. 13. The higher-order diagrams for the four-particle scattering amplitude. Both diagrams are expected to be suppressed (see the text).

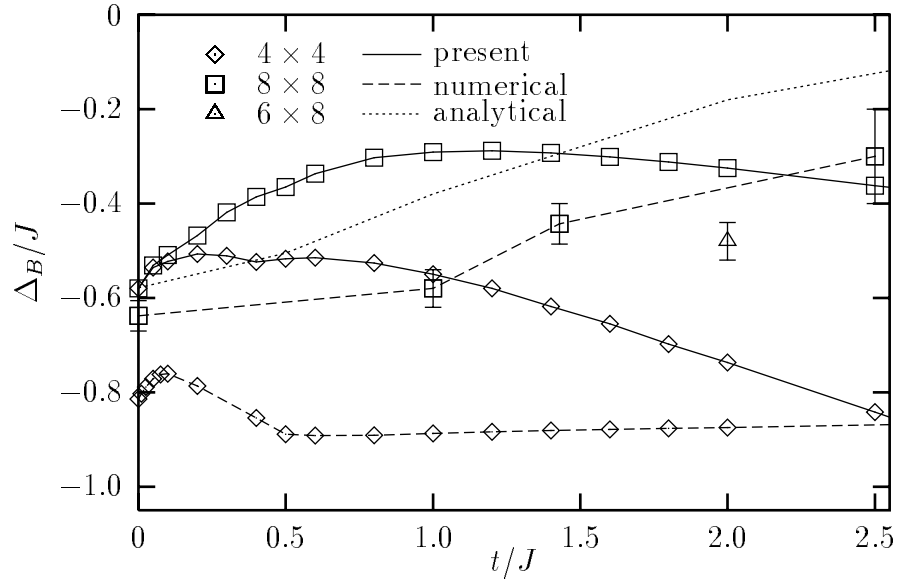


FIG. 14. The two-hole binding energy Δ_B as a function of t/J . The numerical results on the 4×4 lattice are from exact diagonalizations. The numerical results on the 8×8 lattice are from Monte Carlo studies (Barnes and Kovarik¹² for $t/J = 0$ and Boninsegni and Manousakis¹³ for the other points). The numerical result on the 6×8 lattice was quoted by White and Scalapino¹⁴ in a density matrix renormalization group study. The analytical result is from Ref. 15. The irregularities at small t/J on the 4×4 lattice are caused by level crossings (at $t/J = 0.4814$ and 0.1526 , see Ref. 9).

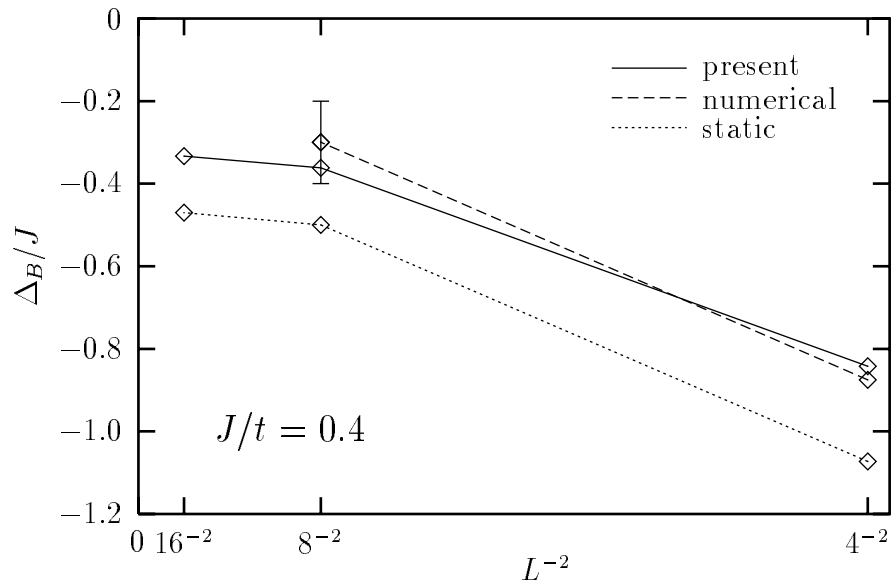


FIG. 15. Size dependence of the two-hole binding energy Δ_B at $J/t = 0.4$. $L \times L$ is the lattice size. The dotted line is the result obtained using the static approximation described in the text.

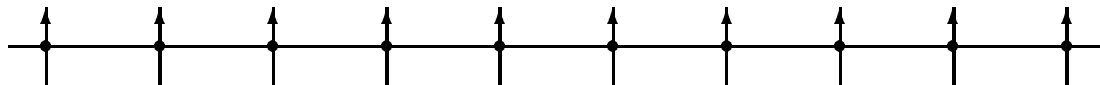


FIG. 16. The perfectly antiferromagnetic ground state.

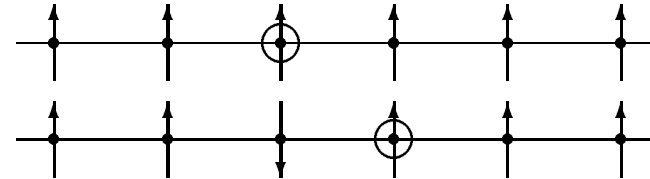


FIG. 17. Motion of a holon in perfectly antiferromagnetic background.



FIG. 18. An antiferromagnetic ground state with spin fluctuations present.

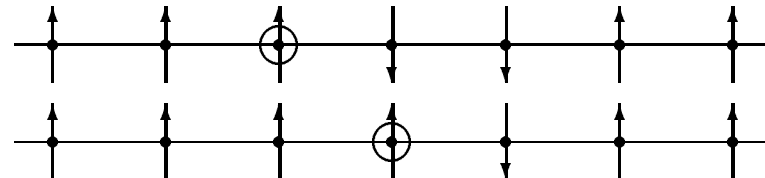


FIG. 19. Motion of a holon encountering a ground-state spin fluctuation.

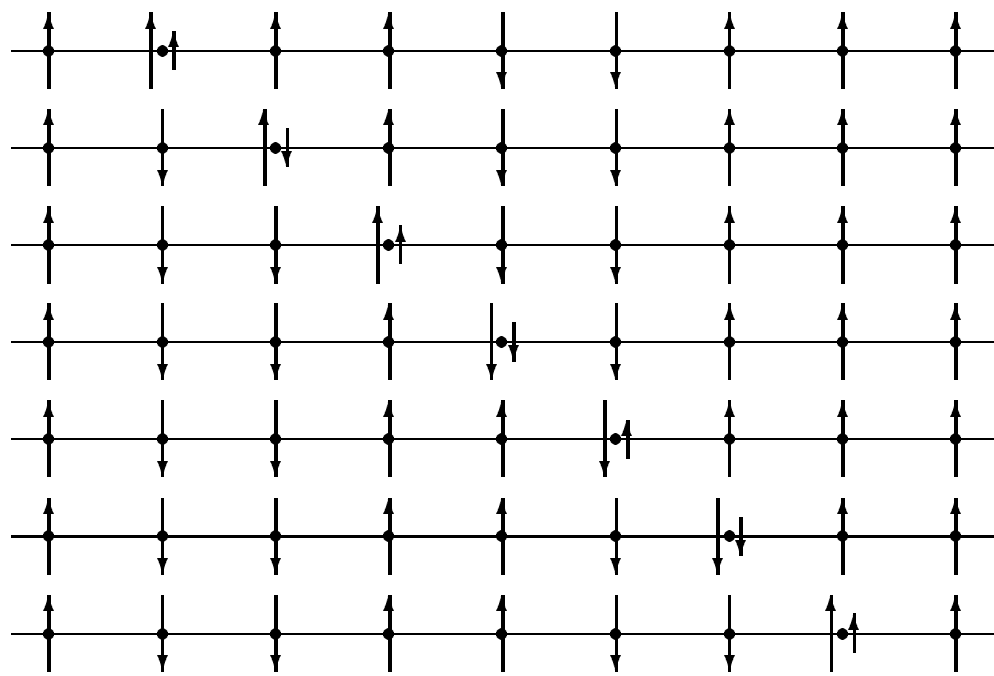


FIG. 20. Motion of a hole in a background with spin fluctuations, as interpreted in the hole-and-slave-spin representation.